Supporting Information

High Capacity for Mg^{2+} Deintercalation in Spinel Vanadium Oxide Nanocrystals

*Linhua Hu[1,2], Jacob R. Jokisaari[3], Bob Jin Kwon[2,5], Liang Yin[2,4], Soojeong Kim[2,4], Haesun Park[2,6], Saul H. Lapidus[2,4], Robert F. Klie[2,3], Baris Key[2,5], Peter Zapol[2,6], Brian J. Ingram[2,5], John T. Vaughey[2,5], Jordi Cabana[1,2]**

[1]Department of Chemistry, University of Illinois at Chicago, Chicago, IL 60607, USA.

[2]Joint Center for Energy Storage Research, Argonne National Laboratory, Lemont, IL 60439, USA.

[3]Department of Physics, University of Illinois at Chicago, Chicago, IL 60607, USA.

[4]X-ray Science Division, Advanced Photon Source, Argonne National Laboratory, Lemont, IL 60439, USA.

[5]Chemical Sciences and Engineering Division, Argonne National Laboratory, Lemont, IL 60439, USA.

[6]Materials Science Division, Argonne National Laboratory, Lemont, IL 60439, USA.

* E-mail: jcabana@uic.edu

Experimental Section

Synthesis

Magnesium vanadium oxide (MVO) nanocrystals were synthesized via a hydrothermal process. 1mmoL magnesium acetate and 2mmoL vanadium chloride were dissolved in 50mL water, followed by dropwise addition of 50mM NaOH solution and 5mL water with stirring. The resultant pH was ~9. Subsequently, the resulting black solution was transferred into an autoclave lined with polytetrafluoroethylene (PTFE), sealed and heated for 12 hours at 120^{o}C. The resultant product was centrifuged and washed with water several times. Finally, the black power was dried overnight at 60^{o}C and calcined at 400^{o}C for 4hours in 5%H_2/95%Ar.

Physical-chemical characterization of the electrodes

High-resolution synchrotron X-ray powder diffraction were performed at beamline 11-BM-B of Advanced Photon Source, Argonne National Laboratory (λ = 0.4127Å). Pawley refinements were performed using GSAS II.[1] Scanning transmission electron microscopy (STEM) was performed using an aberration-corrected microscope (JEOL, Model JEM-ARM200CF) operated at 200 kV. Energy-dispersive X-ray (EDX) data were collected using a high-solid angle Oxford X-MaxN 100TLE silicon drift detector. Only the contents of magnesium and vanadium will be shown for clarity. Magnesium/vanadium ratio was evaluated by EDX with multiple selected area for different electrodes. Elements analysis was performed on Thermo iCAP 7600 Inductively Coupled Plasma Optical Emission Spectroscopy (ICP-OES) with dual view (Radial and Axial) optical emission spectrometer.

Solid-state ^{25}Mg magic angle spinning (MAS) NMR experiments were performed at 11.7 Tesla (500 MHz) on a Bruker Advance Ⅲ spectrometer operating at a Larmor frequency of 30.64 MHz using a 3.2 mm MAS probe. The spectra were acquired at a spinning speed of 20 kHz with

a recycle delay of 0.5 second for 3.2mm rotors with a rotor synchronized spin-echo experiment (90°-τ-180°-τ) where τ is 1/r. All ^{25}Mg shifts were referenced to 5 M $MgCl_2$ (aq.) at 0 ppm.

V K-edge X-ray absorption spectroscopy (XAS) measurements were performed at the MRCAT bending magnet 10-BM beamline at the Advanced Photon Source, Argonne National Laboratory. X-ray absorption spectra were collected in transmission mode through composite electrode laminates. A Si(311) water-cooled double-crystal monochromator was used to scan incident X-ray and scanned energies were detuned by 50 percent. The beam profile was collimated to 3 × 0.75 mm. A V reference foil was measured simultaneously with every sample for energy calibration (V *K*-edge set to 5645 eV). V $L_{2,3}$- and O *K*-edge XAS measurements were performed at beamline 4-ID-C at the Advanced Photon Source, Argonne National Laboratory. Spectra were obtained at a resolution of ~0.2 eV using detectors of the total electron yield (TEY) and total fluorescence yield (TFY).

Room Temperature synchrotron X-ray total scattering data were collected on beamline 11-ID-B, the Advanced Photo Source, Argonne National Laboratory. The rapid-acquisition PDF method was used with an X-ray energy of 58.6 k eV (λ = 0.2113 Å).[2] A PerkinElmer amorphous Si two-dimensional image-plate detector (2048 × 2048 pixels and 200 × 200 μm pixel size) was used at a distance of ~180 mm. The two-dimensional data were converted to one-dimensional XRD data using the GSAS-II software. PDF data were obtained from Fourier transformation of the background and Compton scattering corrected data *S(Q)* in *xPDFsuite* software over a *Q* range of 0.1-22.5 Å^{-1}.[3-4]

XPS experiment was carried out by Kratos Axis-165 surface analysis system with a Monochromatic Al source. Charge neutralizer was applied during the experiment to avoid

charging. The energy resolution of the XPS is less than 0.45 eV. For data processing, Shirley background has been applied and XPSPEAK41 software has been used to fit the data.

Electrochemical Measurements

The working electrodes were prepared by mixing the nanocrystal samples, carbon black (Denka), and polyvinylidene difluoride (PVDF) (Kynar) in N-methylpyrrolidone (NMP) (Sigma−Aldrich) (60:20:20 (wt%)), which were then cast on an electrochemical-grade stainless steel 316 mesh using a doctor blade, followed by drying under vacuum at 110 °C overnight. Dried electrodes, with a loading level of ~3 mg/cm^2, were punched with a diameter of 1/2" and assembled into 2032 coin-type cells in an Ar-filled glovebox (water and oxygen, ≤ 0.1 ppm).

Electrochemical half cells contained an activated carbon mesh as a counter electrode, a glass fiber separator (VWR, grade 691, 28297-289) and 0.5 M $Mg[N(SO_2)_2(CF_3)_2)_2$-$(C_9H_{20}N)(N(SO_2)_2(CF_3)_2]$ (abbreviated as $MgTFSI_2$-$PY_{14}TFSI$) with low H_2O content (~43 ppm) as electrolyte. For 2-electrode cells, the potential of cathode was calibrated by considering the AC anode potential, which is originally 2.2 V vs Mg^{2+}/Mg^0 and linearly proportional to the state-of-charge (SoC). Electrochemistry was carried out at 110 °C or 25°C in the potential range 0.6~3.5 V vs Mg^{2+}/Mg^0. [5] The charge/discharge rate (C/20) was galvanostatically controlled by a Bio-Logic VMP3 potentiostat.

Full cells contained a fresh Mg foil as a counter electrode, a glass fiber separator (VWR, grade 691, 28297-289) and 0.1 M $Mg[Al(OC(CF_3)_3)_4]_2$ dissolved in triglyme (abbreviated as $Mg(TPFA)_2$ as electrolyte.[6] Electrochemistry was carried out at 85 °C in the potential range 0.25~3.8 V vs Mg^{2+}/Mg^0 . The charge/discharge rate (C/20) was galvanostatically controlled by MACCOR battery cycler. After oxidation or reduction of the MgV_2O_4 electrodes, they were

recovered and rinsed in acetonitrile three times, and dried at room temperature under vacuum for 1 minute before characterization. Samples were harvested at the end of charge, and at 2V, 1.7V, 1.2V and 0.9V upon discharge. They are listed as Charge, Dis 2V, Dis 1.7V, Dis 1.2V, Dis 0.9V.

Density Functional Theory Calculations

The Mg migration barriers in MgV_2O_4 spinel framework are calculated using density functional theory as implemented in Vienna Ab initio Simulation Package (VASP).[7-8] The projector-augmented wave (PAW) potential method was used to describe the core-valence electron interactions.[9-10] The plane-wave cuff-off energy was set to 550 eV. The generalized gradient approximation (GGA) method formulated by Perdew-Burke-Ernzerhof (PBE) was used to express the exchange-correlation energy in Kohn-Sham equation.[11-12] The Brillouin zone was sampled using a Monkhorst-Pack scheme with a Γ-centered k-point mesh of 2×2×2. The minimum energy pathway for Mg migration in spinel structure was obtained by nudged elastic band (NEB) method where a 2×2×2 supercell of the spinel primitive cell was used to avoid the interaction between the migrating Mg atoms in periodic images.[13] We considered the two extreme Mg concentration cases: (i.) a single Mg in the empty V_2O_4 spinel structure (high vacancy concentration limit) and (ii.) a single Mg vacancy in the MgV_2O_4 spinel (dilute vacancy concentration limit). Due to the difficulty in converging NEB calculations, the Hubbard U correction was excluded in migration calculations as suggested in previous study.[14]

References

1. Toby, B. H.; Von Dreele, R. B., GSAS-II: the genesis of a modern open-source all purpose crystallography software package. *J. Appl. Crystallogr.* **2013,** *46*, 544-549.

2. Chupas, P. J.; Qiu, X.; Hanson, J. C.; Lee, P. L.; Grey, C. P.; Billinge, S. J., Rapid-acquisition pair distribution function (RA-PDF) analysis. *J. Appl. Crystallogr.* **2003,** *36*, 1342-1347.

3. Yang, X.; Juhas, P.; Farrow, C. L.; Billinge, S. J., xPDFsuite: an end-to-end software solution for high throughput pair distribution function transformation, visualization and analysis. *arXiv preprint arXiv:1402.3163* **2014**.

4. Adams, B. D.; Zheng, J. M.; Ren, X. D.; Xu, W.; Zhang, J. G., Accurate Determination of Coulombic Efficiency for Lithium Metal Anodes and Lithium Metal Batteries. *Adv. Energy Mater.* **2018,** *8,* 1702079.

5. Yoo, H. D.; Jokisaari, J. R.; Yu, Y. S.; Kwon, B. J.; Hu, L. H.; Kim, S.; Han, S. D.; Loyez, M.; Lapidus, S. H.; Nolis, G. M.; Ingram, B. J.; Bolotin, I.; Ahmed, S.; Klie, R. F.; Vaughey, J. T.; Fister, T. T.; Cabana, J., Intercalation of Magnesium into a Layered Vanadium Oxide with High Capacity. *ACS Energy Lett.* **2019,** *4*, 1528-1534.

6. Lau, K. C.; Seguin, T. J.; Carino, E. V.; Hahn, N. T.; Connell, J. G.; Ingram, B. J.; Persson, K. A.; Zavadil, K. R.; Liao, C., Widening Electrochemical Window of Mg Salt by Weakly Coordinating Perfluoroalkoxyaluminate Anion for Mg Battery Electrolyte. *Journal of the Electrochemical Society* **2019,** *166*, A1510-A1519.

7. Kresse, G.; Furthmüller, J., Efficient iterative schemes for ab initio total-energy calculations using a plane-wave basis set. *Phys. Rev. B* **1996,** *54*, 11169-11186.

8. Hohenberg, P.; Kohn, W., Inhomogeneous Electron Gas. *Phys. Rev.* **1964,** *136*, B864-B871.

9. Blöchl, P. E., Projector augmented-wave method. *Phys. Rev. B* **1994,** *50* , 17953-17979.

10. Kresse, G.; Joubert, D., From ultrasoft pseudopotentials to the projector augmented-wave method. *Phys. Rev. B* **1999,** *59*, 1758-1775.

11. Perdew, J. P.; Burke, K.; Ernzerhof, M., Generalized Gradient Approximation Made Simple. *Phys. Rev. Lett.* **1996,** *77*, 3865-3868.

12. Kohn, W.; Sham, L. J., Self-Consistent Equations Including Exchange and Correlation Effects. *Phys. Rev.* **1965,** *140*, A1133-A1138.

13. Henkelman, G.; Uberuaga, B. P.; Jónsson, H., A climbing image nudged elastic band method for finding saddle points and minimum energy paths. *J. Chem. Phys.* **2000,** *113*, 9901-9904.

14. Liu, M.; Rong, Z.; Malik, R.; Canepa, P.; Jain, A.; Ceder, G.; Persson, K. A., Spinel compounds as multivalent battery cathodes: a systematic evaluation based on ab initio calculations. *Energy Environ. Sci.* **2015,** *8*, 964-974.

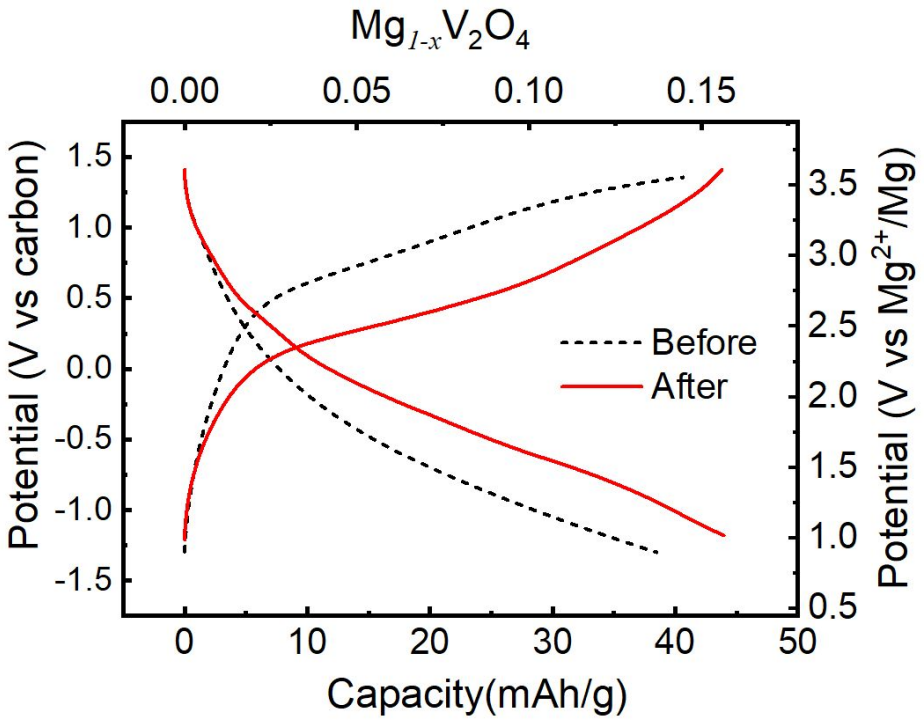

Figure S1. Comparison of voltage profiles collected at 25 °C (C/20 rate), before (black dash line) and after (red solid line) one conditioning cycle at 110 °C.

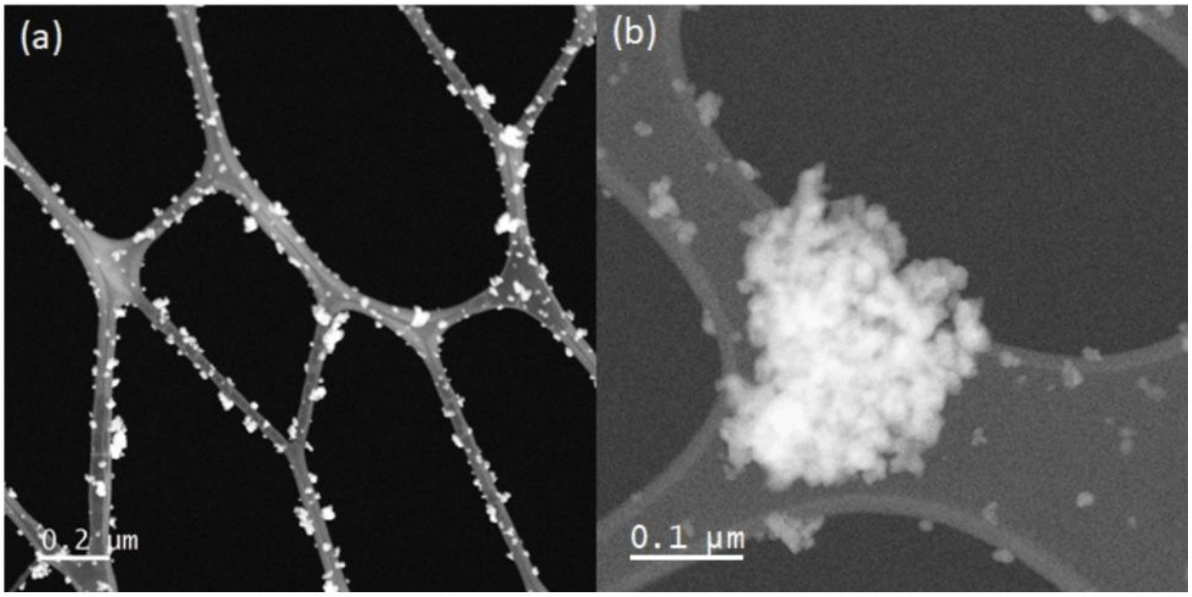

Figure S2. (a) Representative image of nanoparticles dispersed on carbon film with low magnification, (b) a secondary aggregate of many MgV_2O_4 primary sub-5nm nanoparticles.

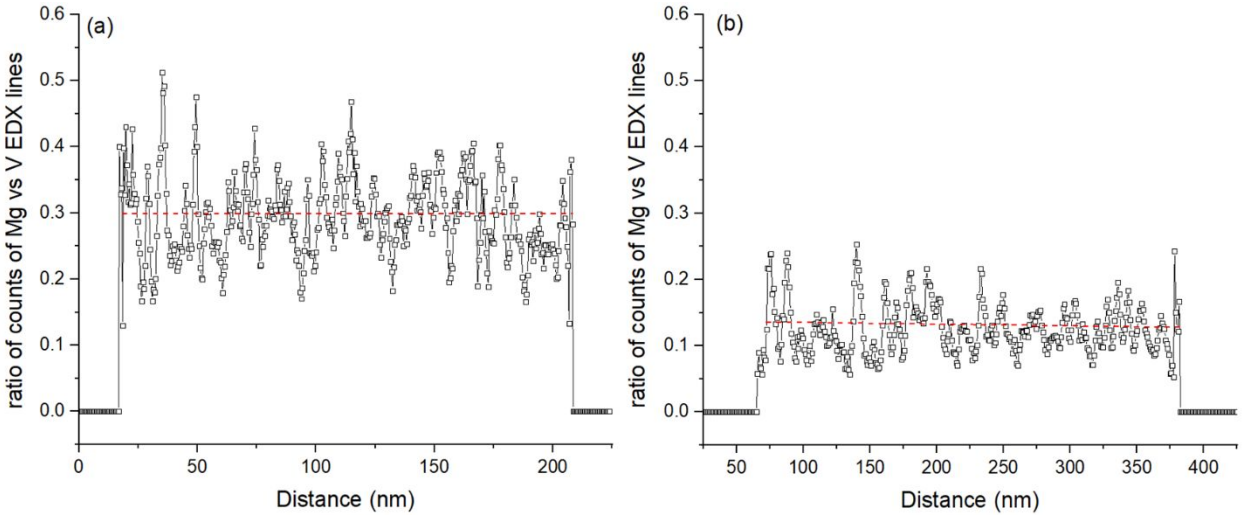

Figure S3. Evolution of the ratio between the intensity of Mg and V K lines along the EDX scans in Figure 3. The red lines indicate the average ratio. (a) Pristine; (b) Charged to 3.4V Mg^{2+} /Mg.

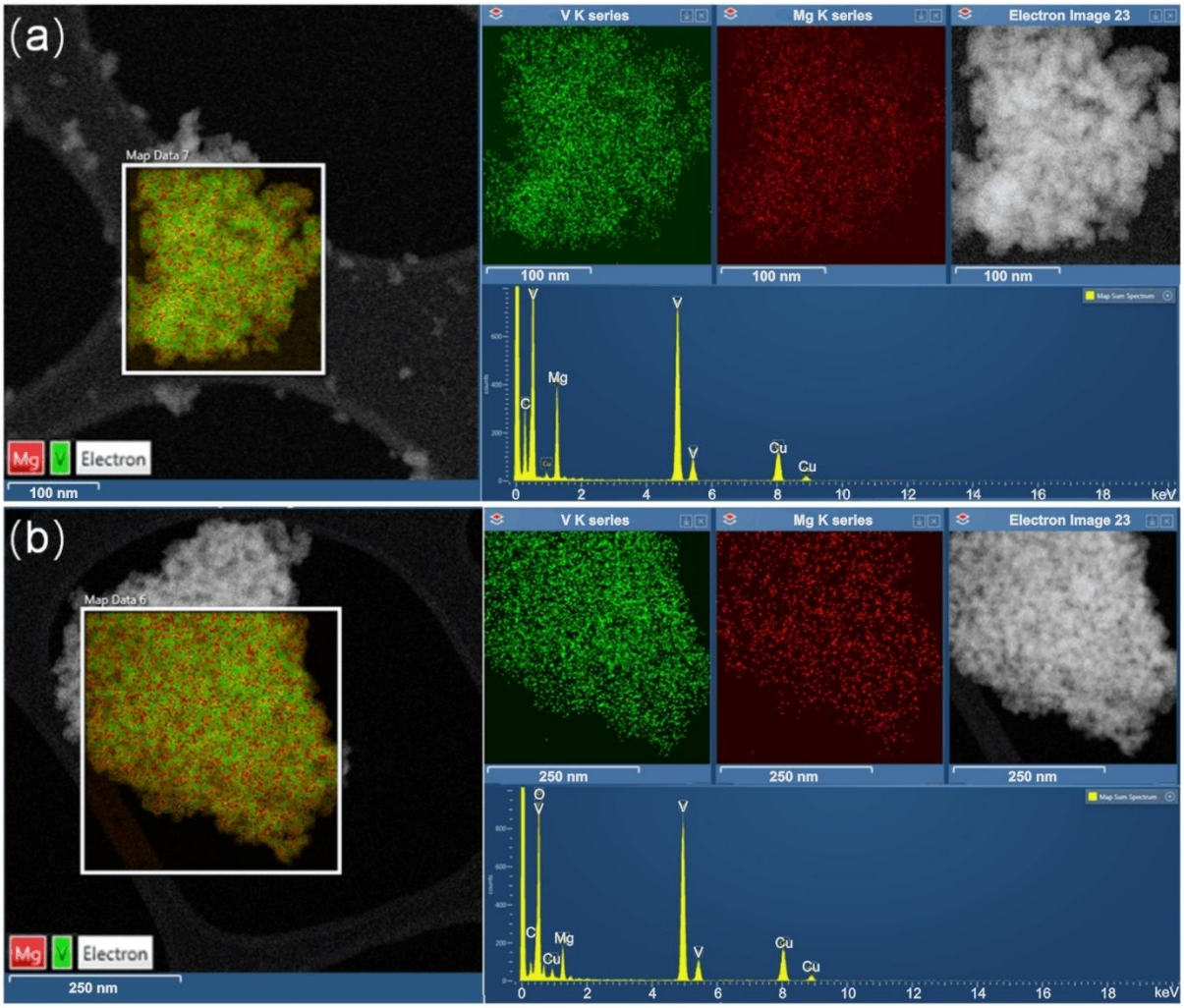

Figure S4 EDX mapping for MVO electrode (a) pristine and (b) charged to 3.4V vs Mg^{2+}/Mg.

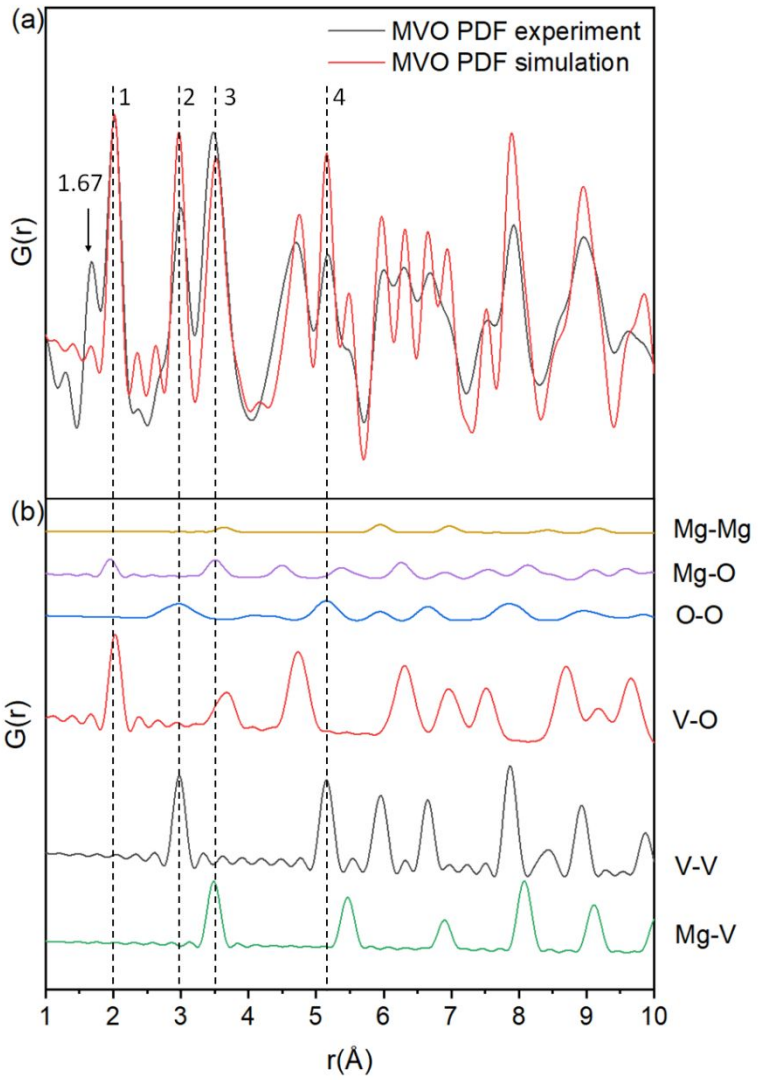

Figure S5. Pair distribution function analysis of MVO nanocrystals (a) experimental and (b) simulated data. The intensity centered at ~2Å (line 1), was the contribution of Mg-O and V-O bonds, and the intensity centered at 3.5Å (line 3), was the contribution of Mg-O and Mg-V bonds, respectively. The experimental intensity of line 1 and 3 is quite close to the simulation result based on standard cubic structure. In contrast, the intensity centered at 3Å (line 2) and 5.2 Å (line 4) was the contribution of O-O and V-V bonds, showing the lower intensity than that of the same simulation. This indicates that V-O and Mg-V bonds are consistent with ideal spinel structure, but V-V and O-O bonds are weaker owing to possible structure defects in frameworks.

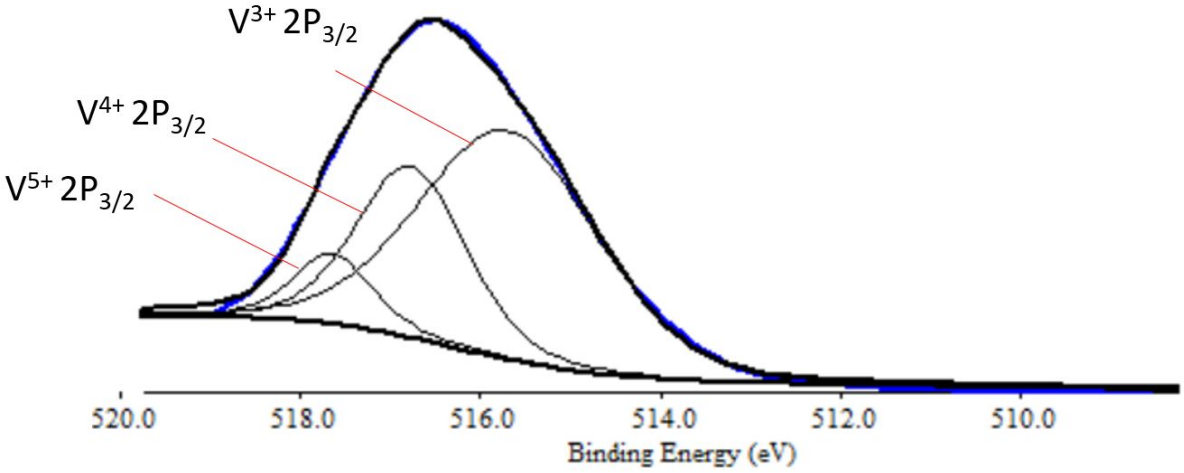

Figure S6. XPS pattern of pristine MgV_2O_4 nanoparticles. A fit of the data revealed the following approximate ratio of oxidation states: V^{3+} : V^{4+} : and V^{5+}, 61% : 30%, : 9%.

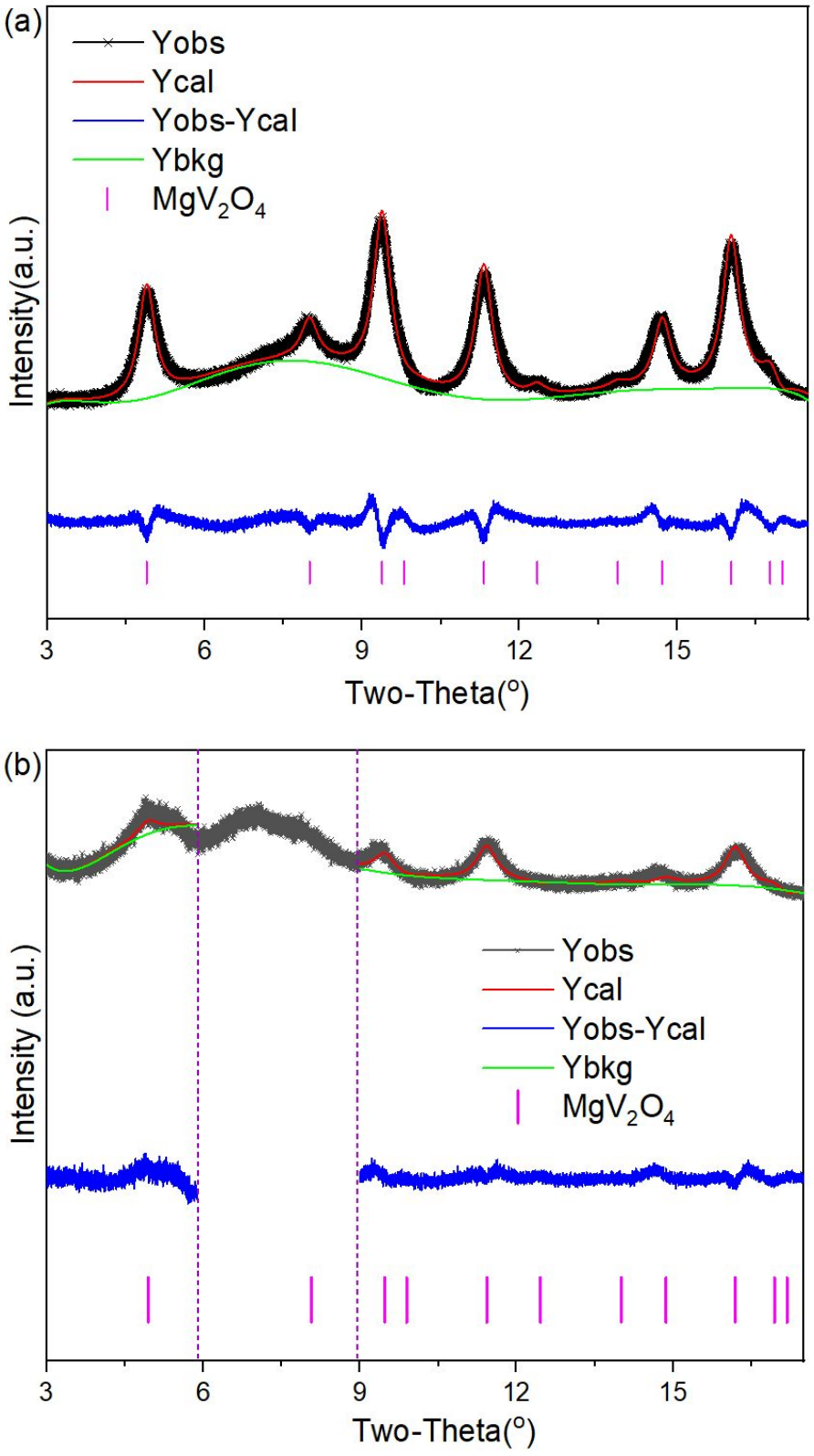
(a)
Yobs
Ycal
Yobs-Ycal
Ybkg
MgV2O4
Intensity(a.u.)
3
6
9
12
15
Two-Theta(°)
(b)
Yobs
Ycal
Yobs-Ycal
Ybkg
MgV2O4
Intensity (a.u.)
3
6
9
12
15
Two-Theta(°)

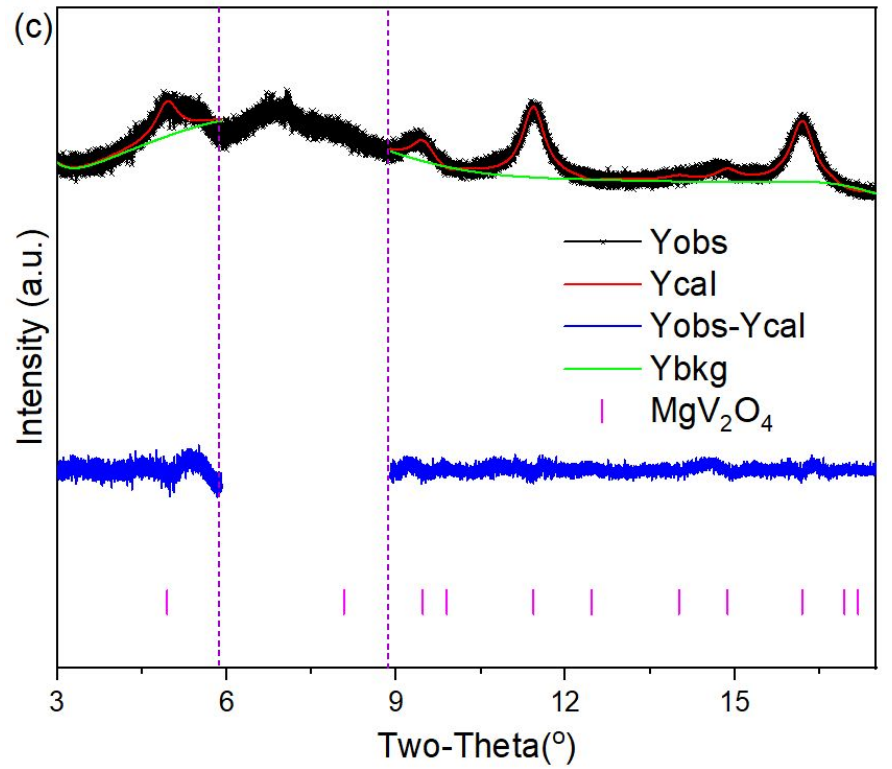
(c)
Intensity (a.u.)
Yobs
Ycal
Yobs-Ycal
Ybkg
MgV2O4
3
6
9
12
15
Two-Theta(°)

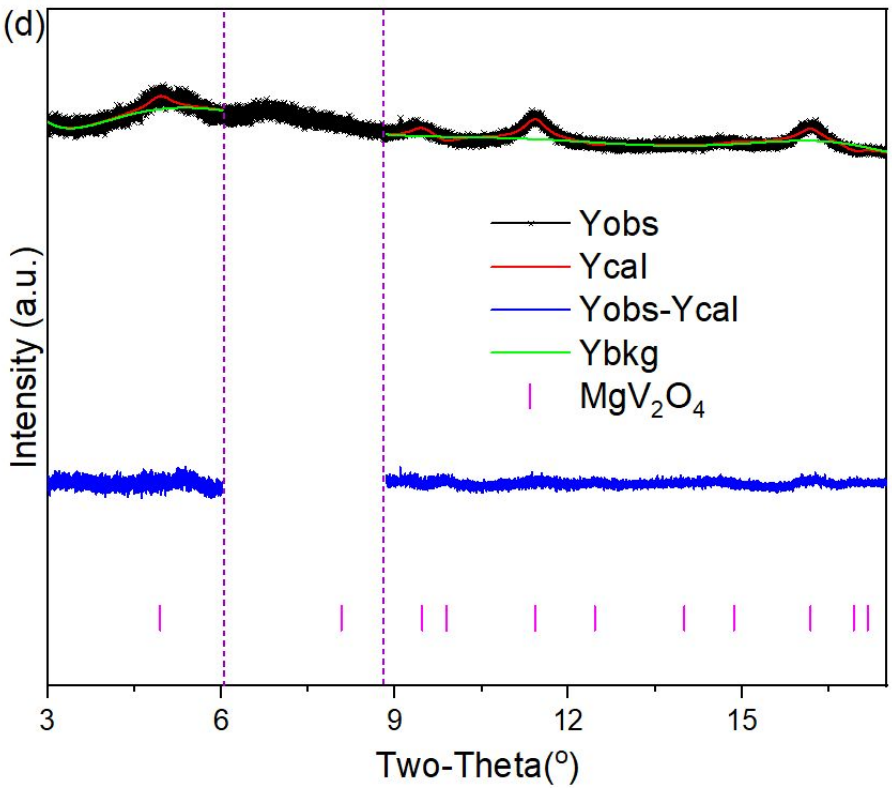
(d)
Intensity (a.u.)
Yobs
Ycal
Yobs-Ycal
Ybkg
MgV2O4
3
6
9
12
15
Two-Theta(°)

Figure S7. Pawley refinements of XRD patterns of different samples performed by high resolution X-ray Diffractometer at beamline 11-ID-B at Advanced Photon Source, Argonne National Laboratory (λ = 0. 4127 Å). (a) Pristine, (b) charged to 3.4V vs Mg^{2+}/Mg^{0}, (c) discharged to 1.7 V vs Mg^{2+}/Mg^{0}, and (d) discharged to 1.2 V vs Mg^{2+}/Mg^{0}. Peaks from carbon black peak were excluded in (b, c, d) by purple dash lines. Black crosses represent the observed intensities. The calculated pattern is shown with red solid line. The difference between the observed and calculated intensities is represented by a blue curve. The background is shown with a green line. Magenta short vertical bars indicate the position of Bragg reflections.

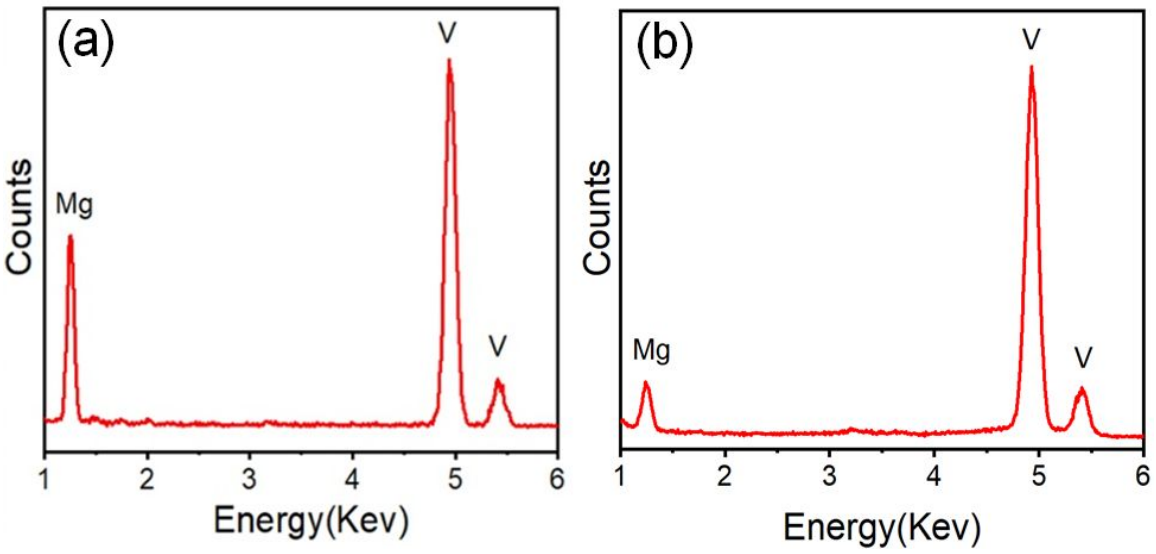

Figure S8. EDX result of Mg and V in (a) Pristine and (b) Charged to 3.5V vs Mg^{2+}/Mg.

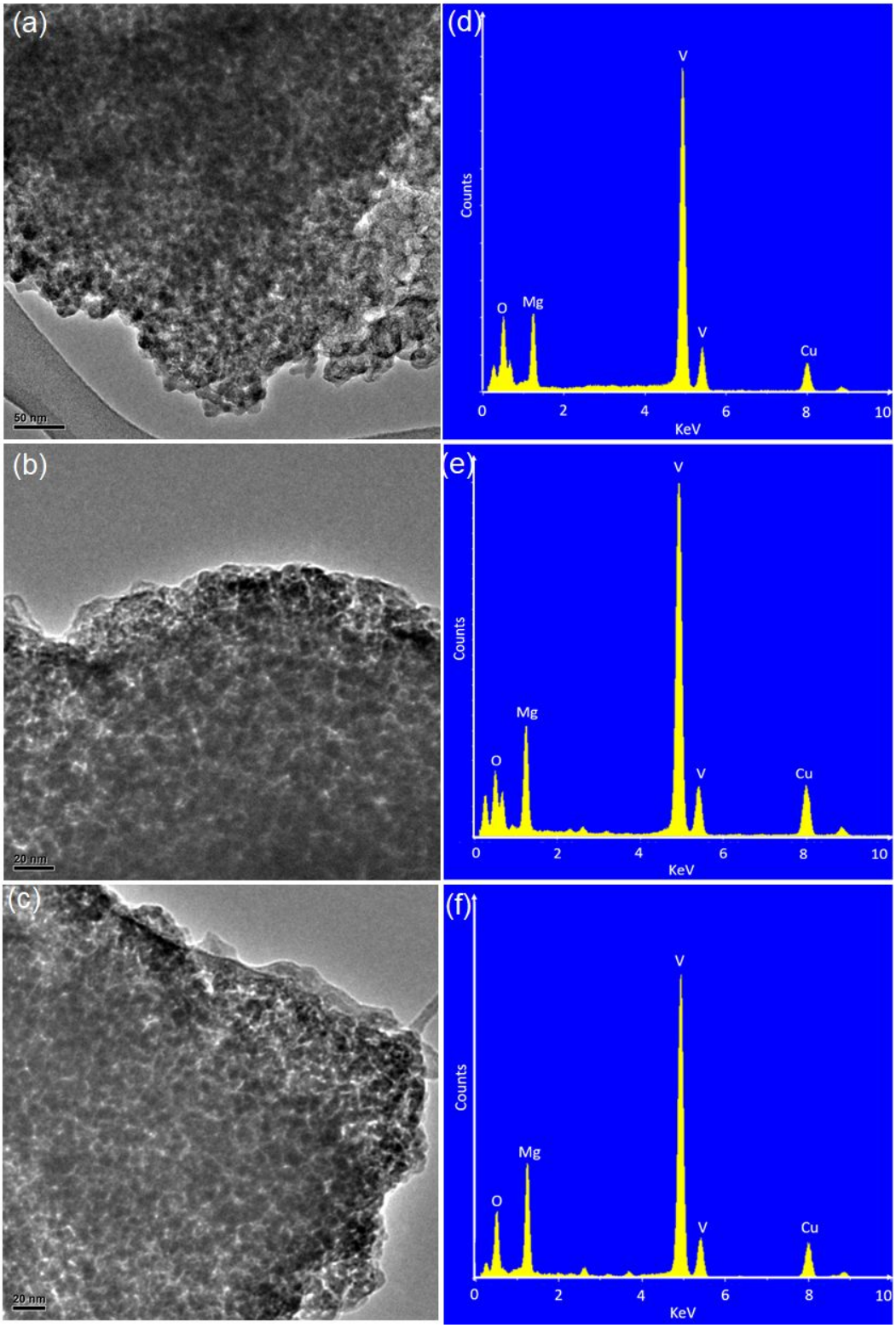

Figure S9. (a, b, c) TEM for MgV_2O_4 NCs of different samples including the electrodes discharged to 1.7V, 1.2V and 0.9V vs Mg^{2+}/Mg^0. (d, e, f) EDX for the corresponding e electrodes discharged to 1.7V, 1.2V and 0.9V vs Mg^{2+}/Mg^0.

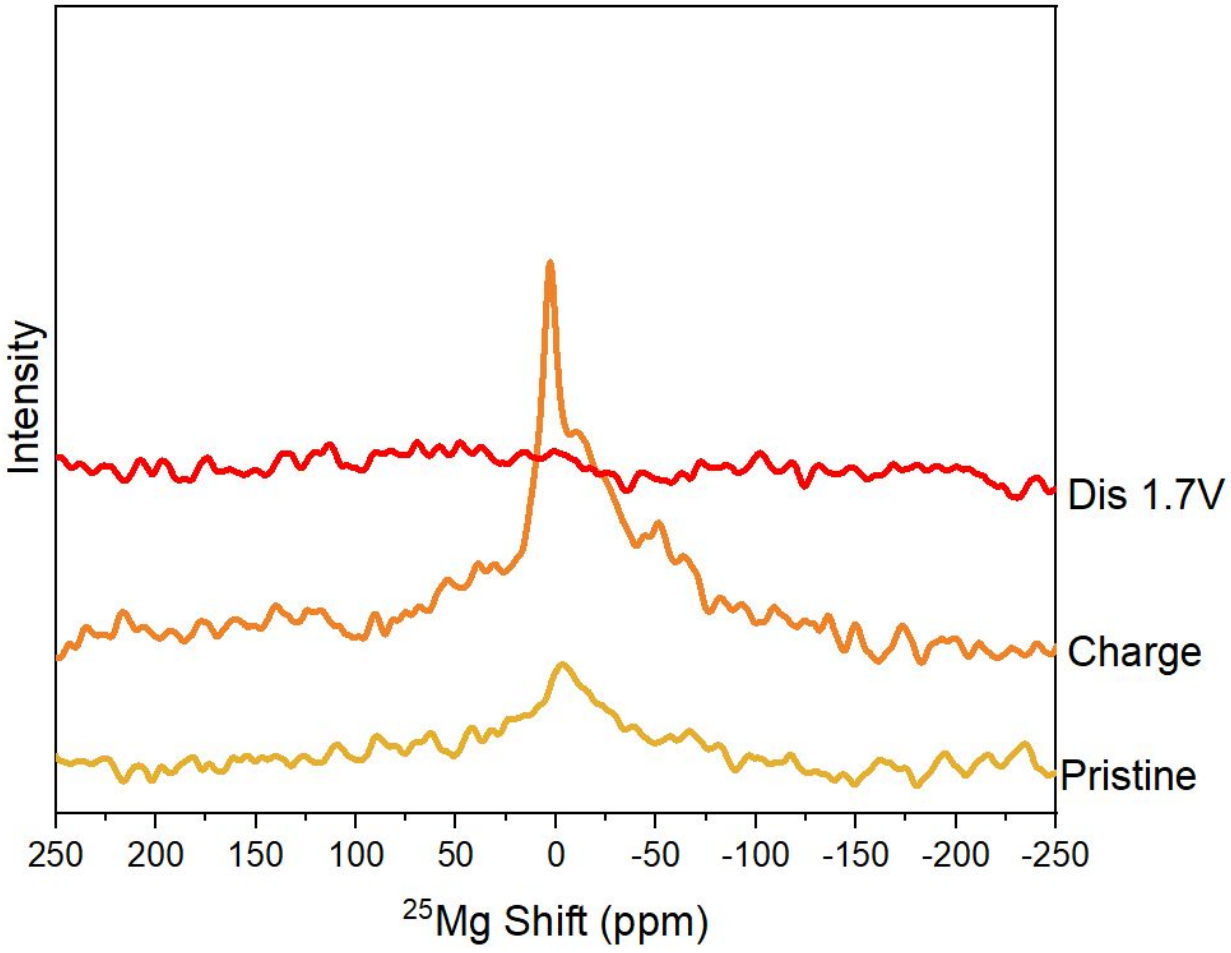

Figure S10. ^{25}Mg NMR spectra in the diamagnetic region of pristine, charged to 3.4V vs Mg^{2+}/Mg, and discharged to 1.7V vs Mg^{2+}/Mg.

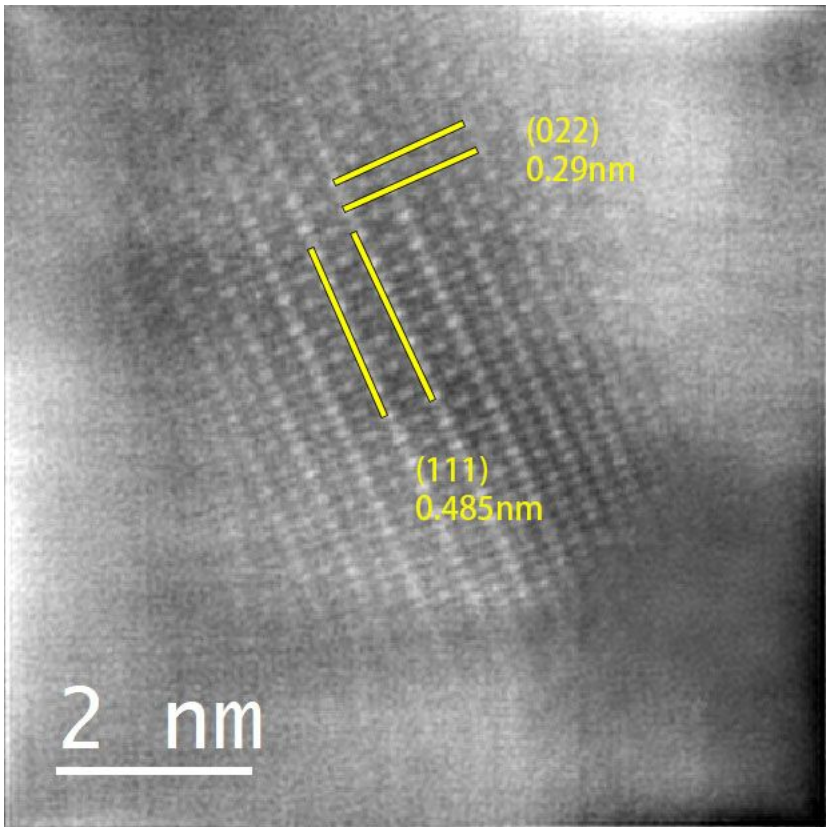

Figure 11. Representative atomic-resolution STEM image of particles harvested from an electrode discharged to 1.7 V vs Mg^{2+}/Mg. The atomic stacks were consistent with the [211] zone axis of the spinel structure. The lattice distance for (022) and (111) are labelled.

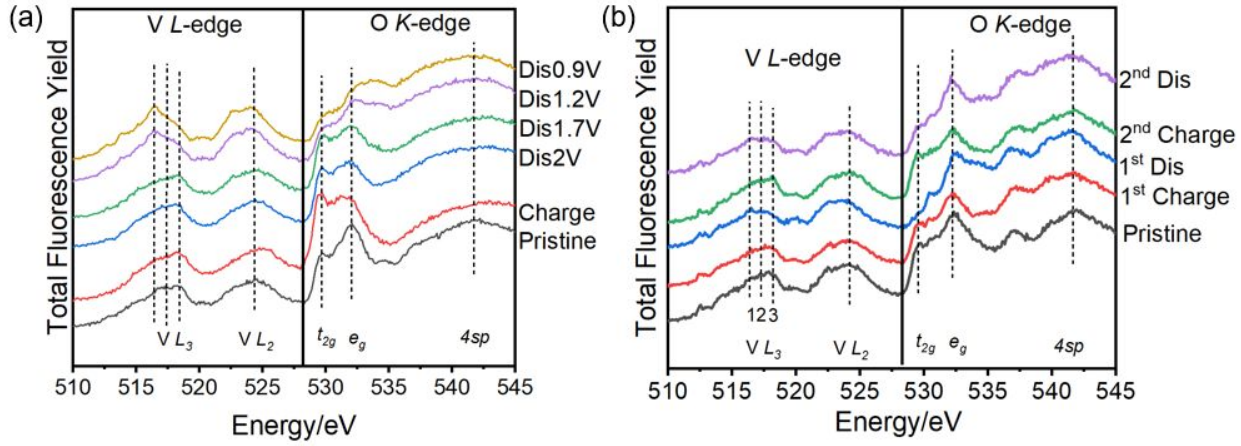

Figure S12. V $L_{2,3}$- and O K-edge XAS collected via TFY detection for electrodes harvested from (a) half cells (b) full cells.